Deepening of the Study of Corona Discharges by Recent Advances of Electrical and Optical Measurement Techniques

S. Kanazawa[1, *], T. Mitsui[1], A. Kuno[1], T. Furuki[1], K. Tachibana[1], R. Ichiki[1], T. Sato[2], M. Kocik[3], J. Mizeraczyk[4]

[1] *Department of Innovative Engineering, Oita University, 700 Dannoharu, Oita, 870-1192, Japan*
[2] *Institute of Fluid Science, Tohoku University, 2-1-1 Katahira, Aoba-ku, Sendai, 980-8577, Japan*
[3] *Institute of Fluid Flow Machinery, Polish Academy of Sciences, Fiszera 14, Gdańsk, 80-231, Poland*
[4] *Department of Marine Electronics, Gdynia Maritime University, Morska 81/87, 81-225, Gdynia, Poland*

Corresponding author*: skana@oita-u.ac.jp*

Abstract. The basic properties and applications of corona discharges have been studied for a long time. The fundamental research covers a wide range of discharge parameters, including corona starting voltage, current values and its distribution, several modes depending on the applied voltage polarity (glow and streamer for positive coronas, Trichel pulse and pulseless glow for negative coronas), ionic wind induced EHD gas flow, and ozone levels. In recent years, we have developed the methodology for the investigation of these all characteristics under repetitive ramp and triangular voltage applications. In particular, recent advances in measurement methods have led to an in-depth the understanding of corona discharges. Here, a typical needle-to-plate electrode system is used as the discharge electrode. The electrical characteristics of both positive and negative corona discharges (e.g., the corona onset voltage, the voltage at which the corona discharge transfers its mode, the appearance of corona discharge modes, the average current-voltage (*I-V*) characteristics, and the corona discharge hysteresis) is automatically investigated by repetitive ramp and triangular voltages generated with a high voltage amplifier with a function generator. Optical study makes clear the corona emission by full color observation with optical emission spectroscopy. Furthermore, real color corona imaging is performed by using a highly sensitive digital camera equipped with a zoom lens. Also the gas velocity flow field generated by ionic wind is observed by Schlieren technique. These extensive research opportunities will further advance our knowledge of corona discharges. This paper presents a broad overview of the latest corona discharge measurement technology we have developed.

Keywords: Corona discharge, Ramp voltage, Automatic measurement, Streamer, Glow, Trichel pulse, Corona emission, EHD

1. Introduction

In recent years, the three major discharges that produce atmospheric pressure non-thermal equilibrium plasmas are corona discharges [1, 2, 3], barrier discharges [4], and plasma jets [5, 6]. Among them, corona discharge is effectively employed for particle charging in electrostatic precipitators (ESPs) [7], as ion sources in ionizers. Streamer corona discharge is used for the removal of harmful particulate matters/gaseous components and the sterilization of microorganisms in air-cleaning ESPs [8]. In addition, scientific challenges in the understanding of corona discharges are exciting because of their several modes depending on the applied voltage polarity. The basic properties and applications of corona discharges have been studied for a long time [1, 2, 3, 7, 8]. Experiments dealing with the corona discharge date back more than 100 years ago. Many early studies by Japanese researchers, especially those published in Japanese, have been little known, with a few exceptions [9, 10]. We have been studying corona discharges for more than 30 years. In particular, recent advances in measurement methods have led to an in-depth the understanding of corona discharges. Our group found that ramped and triangular voltages enabled us to investigate the electrical characteristics of corona discharges more easily and quickly than DC voltage [11]. In the past, some characteristics of the corona discharge (e.g., the corona onset voltage, the transition voltages of the discharge modes, and the hysteresis of the corona discharge) were measured by changing the DC voltage manually and slowly, but such measurement was time consuming [12, 13]. To improve this measurement procedure, the repetitive ramped and triangular voltages instead of the DC voltage were used, and we found that these voltages were more useful than the DC voltage to obtain the characteristics of corona discharges. Our optical study includes the laser-induced fluorescence (LIF) and optical emission spectroscopy (OES) to detect the molecules such as NO [14, 15], N_2 metastable [16, 17] and OH radicals [18, 19]. Furthermore, real color corona imaging is performed by using a highly sensitive digital camera equipped with a zoom lens. Also the gas velocity flow field, electrohydrodynamic (EHD) effects, generated by ionic wind is observed by Schlieren and PIV techniques [20, 21]. These extensive research opportunities will further advance our knowledge of corona discharges. This paper presents a broad overview of the latest corona discharge measurement technology we have developed.

2. Experimental Setup

Fig. 1 shows a schematic diagram of an experimental setup. We generated the corona discharge between a needle electrode and a plate electrode. The needle electrode, which was made of tungsten and had a curvture radius of 30 μm, was placed at the center of the plate electrode. The plate electrode was made of brass and had a diameter of 70 mm, and a gap distance between the needle and the plate electrodes was set to 10 mm. We used a function generator (NF, WF1974) and a high voltage amplifier (Trek, Model 20/20A) to generate arbitrary high voltage

waveforms. In our experiment, positive and negative DC and ramped high voltage waveforms were employed. The ramped voltage was varied from 0 V to a peak value linearly within 49 ms and returned from the peak value to 0 V linearly within 1 ms with a repetition frequency of 20 Hz. This high voltage was applied to the needle electrode in order to generate the corona discharge. A ballast resistor (20 MΩ) was inserted between the high voltage amplifier and the needle electrode so that the discharge current would be limited when unexpected breakdown occured between the gap. In order to measure not only pulse currents in streamer or Trichel pulse but also dc component in glow mode, a shunt resister (10 kΩ) was inserted between the plate electrode and the ground to measure the corona discharge current.

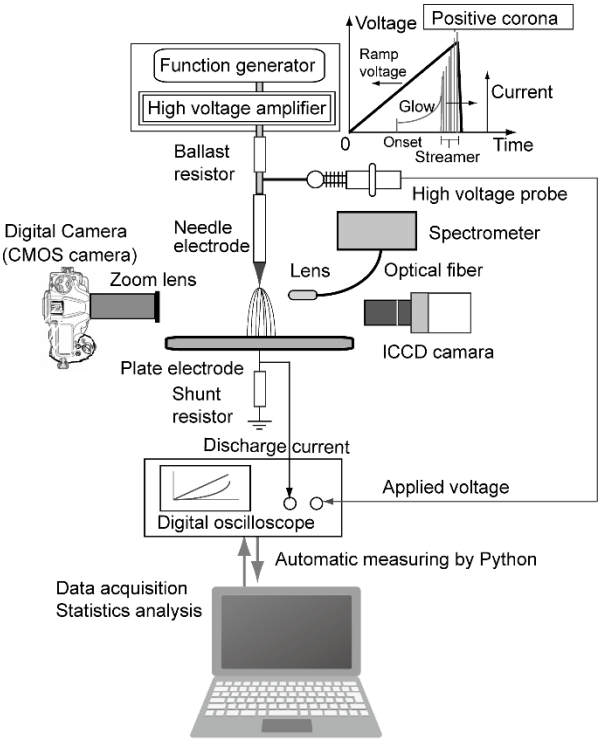

Fig. 1 Schematic diagram of experimental system.

A digital oscilloscope (ROHDE&SCHWARZ, RTA4004) was used to record voltage and current waveforms. The voltage at the needle electrode and the corona discharge current were measured with a high voltage probe (HV-P30, Iwatsu) and the shunt resistor, respectively. Measurement values of the discharge current were obtained by dividing the voltage drop across the shunt resistor by its resistance. Automatic measurement of corona discharge was performed using the Python programming language. Combining this phenomenon-traceable voltage application method with automated measurement, the statistical analysis of corona discharge characteristics was made for more than 100 discharge events under the same

operating condition. The numerical data treatment enables us to determine the corona onset voltage and the transition voltage for glow-to-streamer or Trichel pulse-to-glow as well as those average values and the standard deviations.

Optical emission of the DC corona discharge was observed by using a spectrometer (Ocean Photonics, Maya 2000Pro) with an optical fiber equipped with a convergence lens. We observed the optical emission around the tip of the needle electrode for both the positive and negative polarity. On the other hand, discharge full color images were captured by a digital camera (Nikon, D6) with a zoom lens (KEYENCE, VH-Z50l). Moreover, time-resolved discharge images were captured with an ICCD camera (Andor, iStar DH734) when the ramped voltage was applied. We synchronized the corona discharge with the ICCD camera gate using the function generator, and a delay (t_{delay}) of the ICCD camera gate from the beginning of the voltage increase was controlled to capture an image at the appropriate timing.

The EHD gas flow due to ionic wind was observed by Schlieren method. Fig. 2 shows a schematic of the Schlieren system. The system consists of a high intensity halogen lamp, twin concave mirrors (15 cm in diameter), a kinfe-edge, and the digital camera.

The experiment was carried out at room temperature and under atmospheric pressure. Temperature, relative humidity, and pressure in each experiment were recorded using a thermo recorder (T AND D, TR-73U).

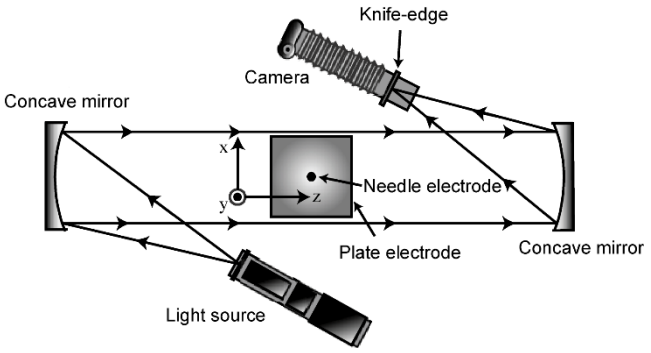

Fig. 2 Schematic diagram of Schlieren system.

3. Results and Discussion

3.1. Discharge characteristics

Fig. 3 shows typical current-voltage (*I-V*) characteristics for positive corona when a DC high voltage was applied to the needled electrode manually. The time-averaged discharge current was measured by a moving-coil type ammeter. Except for the streamer mode in positive corona, *I-V* characteristics can be well fitted by the theoretical formula

$$I = AV(V\text{-}V_{\text{onset}}) \qquad (1)$$

where I, A, V and V_{onset} are the corona current, a constant that is dependent on the experimental conditions, the voltage at the needle electrode and the corona inception voltage, respectively. When a positive glow corona discharge transitions to a streamer corona discharge, the pulse current component becomes larger and I-V curve does not fit the theoretical formula. On the other hand, Fig. 4 shows one example of voltage and current waveforms when we applied positive ramped voltage repeatedly. In this case, we observed large current spikes started to be generated when the voltage was +4.0 kV, indicating a discharge-mode transition from the glow to streamer mode. In order to analysis of streamer onset voltages, the data for voltage and current waveforms of 100 discharge events under the same operating condition was stored into a computer memory. The voltage and current waveforms of the discharges were acquired every second, and the overall measurement time was 10 minutes. Fig. 5 shows the variation and its histogram of streamer onset voltages. Fig. 6 shows typical current-voltage (I-V) characteristics for negative corona when a DC high voltage was applied to the needled electrode manually. The I-V curve of negative corona discharge is well fitted by the theoretical formula. Fig. 7

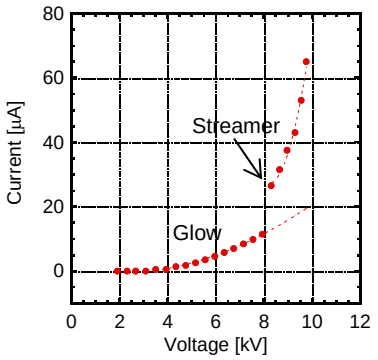

Fig. 3 I-V curve for positive corona.

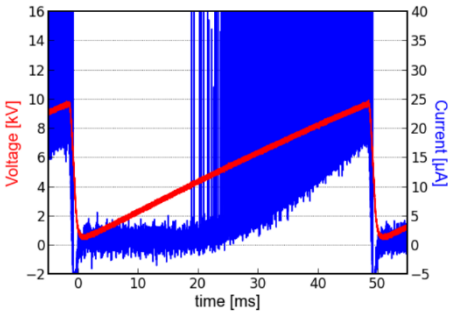

Fig. 4 I-V waveforms for positive corona. (13 ºC, 49%, 1010 hPa)

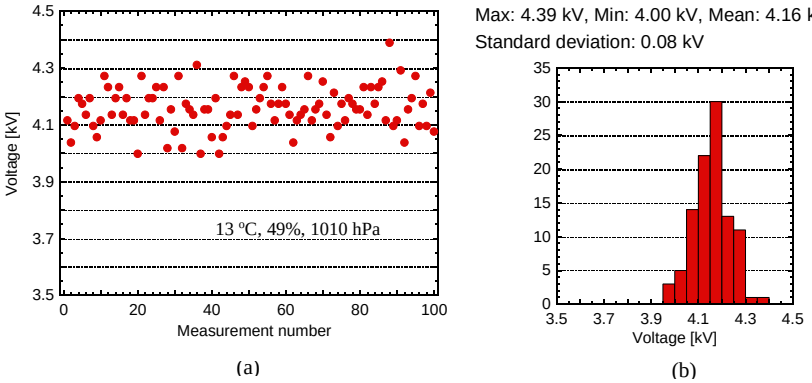

(a) (b)

Fig. 5 (a) Variation of streamer onset voltage and (b) its histogram.

shows one example of voltage and current waveforms when we applied negative ramped voltage repeatedly. In the case of negative polarity, a low of current spikes began to be observed at −3.0 kV, which indicates the generation of the Trichel pulse corona. The peak heights of the current spikes gradually decreased as the voltage increased, and then the current spikes were not observed when the voltage was lower than −6.0 kV, indicating a discharge-mode transition from the Trichel pulse to pulseless glow mode. Figs. 8 and 9 show the variation and the histogram for Trichel pulse onset voltages and transition voltages from Trichel pulse to pulseless glow mode, respectively. These results show that under the same discharge conditions, the variation based on standard deviation is about 2%.

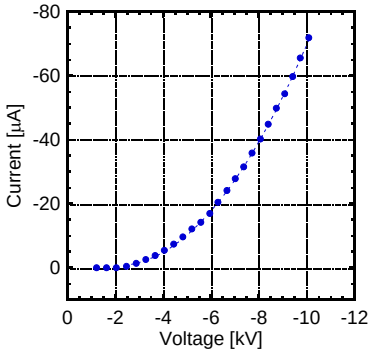

Fig. 6 *I-V* curve for negative corona.

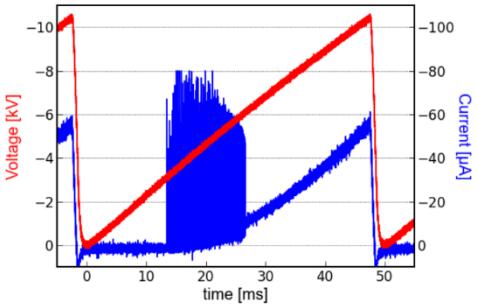

Fig. 7 *I-V* waveforms for negative corona. (13 °C, 47%, 1010 hPa)

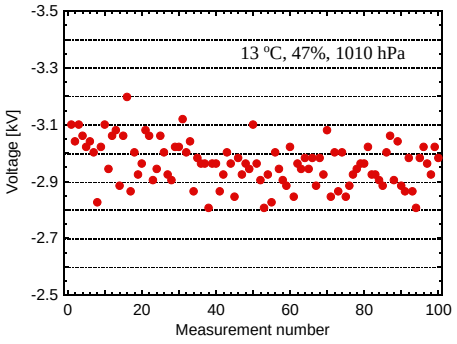

(a)

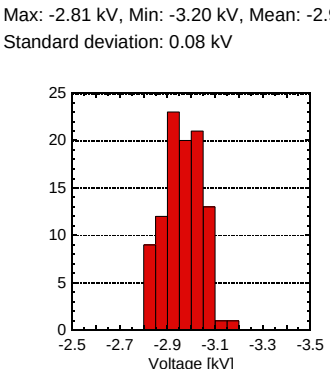

(b)

Fig. 8 (a) Variation of Trichel pulse onset voltage and (b) its histogram.

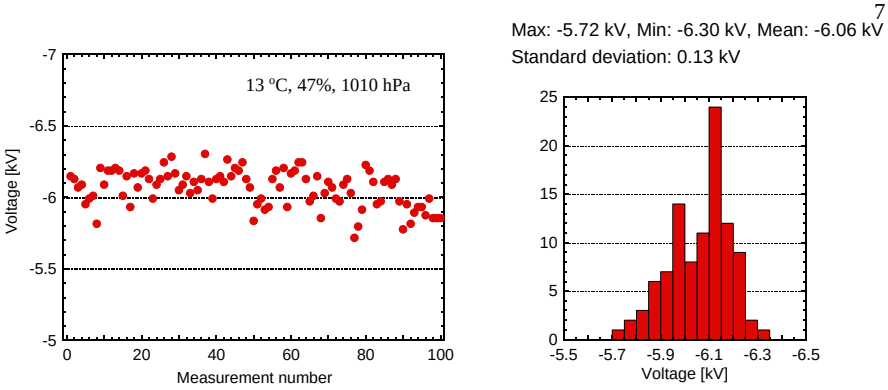

(a) (b)

Fig. 9 (a) Variation of transition voltage from Trichel pulse to pulseless glow mode and (b) its histogram.

3.2. Optical emission characteristics

Fig. 10 shows time-integrated optical emission spectra and full color discharge emission images for the positive DC corona discharges. The spectra were measured with an integration time of 10 s. In the positive glow corona discharge with an applied voltage of +9.4 kV (Fig. 10(a)), we mainly observed peaks in a wavelength range from 290 nm to 430 nm, which are derived from the N_2 2nd positive ($C^3\Pi_u \rightarrow B^3\Pi_u$) and N_2^+ 1st negative ($B^2\Pi_u^+ \rightarrow X^2\Pi_g^+$) systems. In the case of glow corona, faint luminous film-like glow of bluish violet tint is observed in darkness at the tip of the needle electrode. Meanwhile, in the positive streamer corona discharge with an applied voltage of +10.5 kV (Fig. 10(b)), we found some peaks in wavelength ranges of 200 nm–290 nm and 600 nm–900 nm in addition to the peaks corresponding the N_2 2nd positive and N_2^+ 1st negative systems. According to the literature, the peaks in the wavelength ranges of 200 nm–290 nm and 600 nm–900 nm are derived from transitions of nitric oxide (NO) ($A^2\Sigma^+ \rightarrow X^2\Pi$) and the N_2 1st

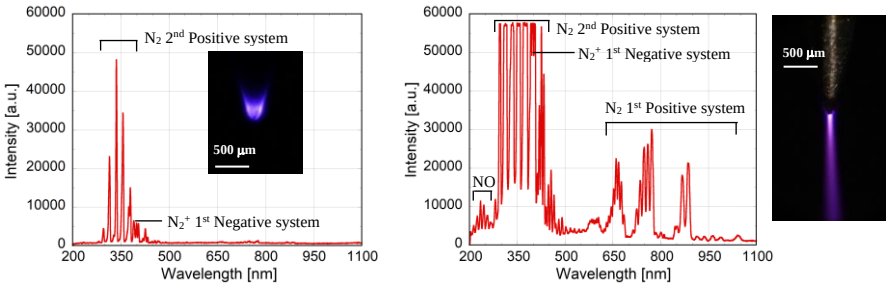

(a) (b)

Fig. 10 Emission spectra of (a) glow mode (9.4 kV) and (b) streamer mode (10.5 kV).

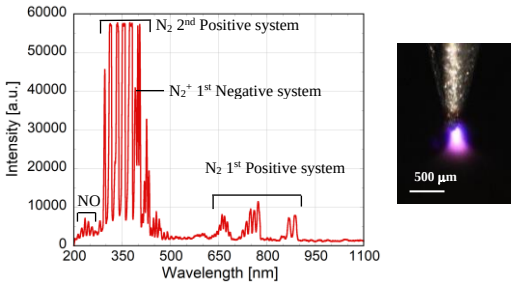

Fig. 11 Emission spectrum of pulseless glow mode (-10.7 kV).

positive system ($B^3\Pi_g \rightarrow A^3\Sigma_u^+$), respectively [22]. When this glow transits to streamer mode, a brilliant reddish streamer channel passes though the gap. The colors of the observed discharges reflect the emission spectra. Those discharge images could not be observed in the ISO sensitivity range that a normal digital camera can set. Fig. 11 shows time-integrated optical emission spectrum for the negative pulseless glow corona and the full color discharge emission image for the negative pulseless glow corona discharge, respectively. The optical emission spectrum for the negative glow corona discharge was similar to that for the positive streamer corona discharge. However, the negative corona emission is characterized by its fan-like spread as shown in Fig.11. The characteristics of the discharge luminescence shown here have been described in black-and-white photographs and sketches in previous literature [1, 2], but in this study they are captured for the first time in color photographs.

3.3. EHD characteristics

Fig. 12 shows typical Schlieren image under the positive DC glow corona discharge at steady state. The downward airflow, i.e. ionic wind, is generated on the axis near the tip of the needle electrode. This airflow gradually changes to more radial directional flow next to the surface of the plate electrode. This change in airflow direction and airflow into the needle electrode generates a doughnut-shaped circulating EHD airflow, which is difficult to see in Fig.12 because of the image

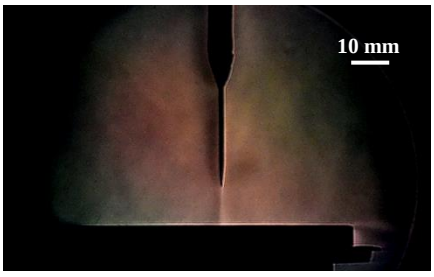

Fig. 12 Schlieren image of glow corona. (8 kV, 20 °C, 38%, 1010 hPa)

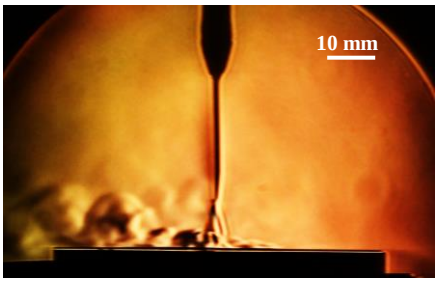

Fig. 13 Schlieren image of streamer corona. (14 kV, 18 °C, 45%, 1013 hPa)

was taken during steady state operation. The observed airflow is consistent with the simulation predictions [20]. While the airflow due to the streamer corona discharge is more violent as shown in Fig.13. The image was taken immediately after the transition from the glow to streamer. This transition has increased the discharge power by a factor of 10 or more. Recently, transition phenomena after the application DC high voltage have been investigated using a high-speed particle image velocimetry and Schlieren visualization [24, 25].

4. Conclusion

This study shows that corona discharges are an old and new field of research. The method we have developed of applying ramped voltage enables observation of discharge phenomena from the start of corona discharge to just before spark discharge all at once. In particular, it is characterized by the fact that it can quickly acquire the many discharge data needed for statistical analysis by repeatedly generating discharges under the same conditions. The discharge generated by this voltage application method are distinct from DC discharge, AC discharge, and pulsed discharge that have been sped up to the nanosecond order, and provide a new means of measurement. We are currently planning to obtain data under a variety of environmental conditions in which corona discharge are used to create a mapping, or what we can call a discharge diagram, of corona discharges.

Regarding EHD characteristics, the flow field generated by a corona discharge is much different from that generated by a barrier discharge, and different fluid control can be expected to be realized [26]. For example, local area cooling by using fine needle electrode, drying enhancement of bulk material with arbitrary shapes by using electrode system consisted of multi-needle-to-mesh electrodes, and treatment/processing by discharge-induced chemical reactions are possible.

ACKNOWLEDGMENT

This work was partly supported by the Japan Society for the Promotion of Science (JSPS) (No. 21H01316).

References

1. Loeb, L. B.: Electrical Coronas. University of California Press, Berkeley and Los Angeles (1965)
2. Meek, J. M., Craggs, J. D., Electrical Breakdown of Gases. John Wiley & Sons (1978)
3. Chang, J.S., Lawless, P. A., Yamamoto, T.: Corona Discharge Processes. IEEE Trans. Plasma Sci. 19, 1152-1161 (1991). doi:10.1109/27.125038

4. Eliasson B., Kogelschatz U.: Nonequilibrium Volume Plasma Chemical Processing, IEEE Trans. Plasma Sci. 19, 1063-1077 (1991). doi:10.1109/27.125031
5. Koinuma H., Ohkubo H., Hashimotto T.: Development and application of a microbeam plasma generator. Appl. Phys. Lett. 60, 816 (1992). doi:10.1063/1.106527
6. Teschke M., Kedzierski J., Finantu-Dinu E. G., Korzec D., Engemann J.: High-Speed Photographs of a Dielectric Barrier Atmospheric Pressure Plasma Jet. IEEE Trans. Plasma Sci. 33, 310-311 (2005). doi:10.1109/TPS.2005.845377
7. White, H. J.: Industrial Electrostatic Precipitation, Pergamon Press, Oxford (1963)
8. Chang J.-S., Kelly A. J., Crowley J. M.: Handbook of Electrostatic Processes, Marcel Dekker, Inc., New York (1995)
9. Nakaya U., Yamasaki F.: Investigations on the Preliminary Stages of Spark Formation in various Gases by the use of the Wilson Chamber, Proc. Roy. Soc., 153, 542-554 (1936) doi:10.1098/rspa.1936.0021
10. Miyoshi Y., Hosokawa T.: The formation of a positive corona in air. J. Phys. D: Appl. Phys., 6, 730-733 (1973). doi: 10.1088/0022-3727/6/6/315
11. Tachibana K., Koshiishi, T., Furuki T., Ichiki R., Kanazawa S., Sato T., Mizeraczyk J.: A new measurement method of DC corona-discharge characteristics using repetitive ramp and triangular voltages. J. Electrostatics. 108, 103525 (2020). doi: 10.1016/j.elstat.2020.103525
12. Bian X., Wang L., MacAlpine J. M. K., Guan Z., Hui J., Chen J.: Positive corona inception voltages and corona currents for air at various pressures and humidities. IEEE Trans. Dielectr. Electr. Insul. 17, 63-70 (2010). doi: 10.1109/TDEI.2010.5412003
13. Robledo-Martinez A.: Characteristics of DC corona discharge in humid, reduced density air. J. Electrostatics. 29, 101-111 (1993). doi: 10.1016/0304-3886(93)90099-S
14. Kanazawa S., Ito T., Shuto Y., Ohkubo T., Nomoto Y., Mizeraczyk J., Chang J.-S.: Two-dimensional distribution of ground-state NO density by LIF technique in DC needle-to-plate positive streamer corona during NO removal processing. IEEE Trans. Ind. Applicat. 37, 1663-1667 (2001). doi: 10.1109/28.968176
15. Kanazawa S., Sumi T., Sato N., Ohkubo T., Nomoto Y., Kocik M., Mizeraczyk J., Chang J.-S.: Wide-range two-dimensional imaging of NO density profiles by LIF technique in a Corona Radical Shower Reactor. IEEE Trans. Ind. Applicat. 41, 200-205 (2005). doi: 10.1109/TIA.2004.840983
16. Kanazawa S., Ohno A., Furuki T., Tachibana K., Ichiki R., Suzuki A., Kuroi K., Suzumura K., Motegi K., Kocik M., Mizeraczyk J.: Temporal-spatial distribution of $N_2(A^3\Sigma_u^+)$ metastable molecules in the pulsed positive streamer in the needle-to-plate gap in sub-atmospheric pressure nitrogen. J. Electrostatics, 103, 103419 (2020). doi: 10.1016/j.elstat.2020.103419
17. Kanazawa S., Mizeraczyk J., NakataniT., Kuno A., Furuki T., Tachibana K., Ichiki R., Kocik M.: Implementation of a single-shot LIF technique for 2-D imaging of metastable nitrogen molecules in a discahrge afterglow at

sub-atmospheric pressures. Measurement, 196, 111262 (2022). doi: 10.1016/j.measurement.2022.111262
18. Kanazawa S., Tanaka H., Kajiwara A., Ohkubo T., Nomoto Y., Kocik M., Mizeraczyk J., Chang J.-S.: LIF imaging of OH radicals in DC positive streamer coronas. Thin Solid Film. 515, 4266-4271 (2007). doi: 10.1016/j.tsf.2006.02.046
19. Kanazawa S., Kawano H., Watanabe S., Furuki T., Akamine S., Ichiki R., Ohkubo T., Kocik M., Mizeraczyk J.: Observation of OH radicals produced by pulsed discahrges on the surface of a liquid. Plasma Sources Sci. Technol. 20, 034010 (2011). doi: 10.1088/0963-0252/20/3/034010
20. Shimamoto S., Kanazawa S., Ohkubo T., Nomoto Y., Mizeraczyk J., Chang J.-S.: Flow visualization and current distributions for a corona radicals shower reactor. J. Electrostatics. 61, 223-230 (2004). doi: 10.1016/j.elstat.2004.02.009
21. Mizeraczyk J., Koick M., Dekowski J., Dors M., Podlinski J., Ohkubo, T., Kanazawa S., Kawaski T.: Measurement of the velocity field of the flue gas flow in an electrostatic precipitator model using PIV method. J. Electrostatics, 51-52, 272-277 (2001). doi: 10.1016/S0304-3886(01)00098-5
22. Gessel A. F. H. van, Hrycak B., Jasinski M., Mizeraczyk J., Mullen J. J. A. M. van der., Bruggeman P. J.: Temperature and NO density measurements by LIF and OES on an atmospheric pressure plasma jet. J. Phys. D: Appl. Phys., 46, 095201 (2013). doi: 10.1088/0022-3727/46/9/095201
23. Zhao L., Adamiak K.: EHD flow in air produced by electric corona discharge in pin-plate configuration. J. Electrostatics, 63, 337-350 (2005). doi: 10.1016/j.elstat.2004.06.003
24. Moreau E., Audier P., Orriere T., Benard N.: Electrohydrodynamic gas flow in a positive corona discharge, J. Appl. Phys. 125, 133303 (2019). doi: 10.1063/1.5056240
25. Defoort E., Bellanger R., Batiot-Dupeyrat C., Moreau E.: Ionic wind produced by a DC needle-to-plate corona discahrge with a gap of 15 mm. J. Phys. D: Appl. Phys., 53, 175202 (2020). doi: 10.1088/1361-6463/ab7139
26. Fylladitakis, E. D., Theodoridis, M. P., Moronis, A. X.: Review on the History, Research, and Applications of Electrohydrodynamics, IEEE Trans. Plasma Sci. 42, 358-375 (2014). doi:10.1109/TPS.2013.2297173